

Inclusive heavy flavor jet production with semi-inclusive jet functions: from proton to heavy-ion collisions

Hai Tao Li ^a and Ivan Vitev ^a

^a*Los Alamos National Laboratory, Theoretical Division, Los Alamos, NM, 87545, USA*

E-mail: haitaoli@lanl.gov, ivitev@lanl.gov

ABSTRACT: The past several years have witnessed important developments in the QCD theory of jet production and jet substructure in hadronic collisions. In the framework of soft-collinear effective theory, semi-inclusive jet functions and semi-inclusive fragmenting jet functions have allowed us to combine higher order calculations with resummation of potentially large logarithms of the jet radius, $\ln R$. Very recently, the semi-inclusive jet functions for partons fragmenting into heavy flavor jets were computed by Dai, Kim and Leibovich. In this paper we show how the formalism can be extended to c-jet and b-jet production in heavy ion collisions. The semi-inclusive jet functions for heavy flavor jets in a QCD medium are evaluated up to the next-to-leading order in α_s and first order in opacity. For phenomenological applications, we also consider the inclusion of the cold nuclear matter effects and the jet energy dissipation due to collisional interactions in matter. We present the numerical predictions for the cross sections and the corresponding nuclear modification factors in proton-nucleus and nucleus-nucleus collisions and compare our results to data from the Large Hadron Collider.

Contents

1	Introduction	1
2	Semi-inclusive jet functions for heavy flavor	3
2.1	Jet Functions in vacuum	3
2.2	Medium corrections	5
3	Numerical results	10
4	Conclusions	16

1 Introduction

Jet production is one of the cornerstone perturbative Quantum Chromodynamics (QCD) processes in hadronic collisions [1]. It is characterized by large cross sections and has, thus, been measured with unprecedented precision in comparison to other high energy processes. Observables related to jets have served as precision tests of QCD and as tools to search for new physics. In this work, we restrict our discussion on the inclusive heavy flavor-tagged jet production in proton and heavy-ion collisions, which has been measured at the Large Hadron Collider (LHC) [2–5] and will be measured at the Relativistic Heavy Ion Collider (RHIC) [6] in the near future.

Inclusive jet production is a multiscale problem in both proton-proton (p+p) and heavy ion (p+A, A+A) collisions. The differential jet cross section versus transverse momentum p_T and rapidity η in hadronic collisions is factorized as the convolution of the parton distribution functions (PDFs), the hard kernels, and the semi-inclusive jet functions (SiJFs), or the fragmentation functions to jet [7]:

$$\begin{aligned} \frac{d\sigma_{pp \rightarrow J+X}}{dp_T d\eta} &= \frac{2p_T}{s} \sum_{a,b,c} \int_{x_a^{\min}}^1 \frac{dx_a}{x_a} f_a(x_a, \mu) \int_{x_b^{\min}}^1 \frac{dx_b}{x_b} f_b(x_b, \mu) \\ &\times \int_{z_{\min}}^1 \frac{dz_c}{z_c^2} \frac{d\hat{\sigma}_{ab \rightarrow c}(\hat{s}, p_T/z_c, \hat{\eta}, \mu)}{dvdz} J_{J/c}(z_c, w_J \tan(R'/2), m_Q, \mu), \end{aligned} \quad (1.1)$$

where $f_{a,b}$ denotes the usual PDF for parton a or b , $d\hat{\sigma}_{ab \rightarrow c}(\hat{s}, p_T, \hat{\eta}, \mu)/dvdz$ represents the hard function for the sub-process $ab \rightarrow c$, and $J_{J/c}$ is the jet function describing the probability of a parton c with transverse momentum p_T/z_c to fragment into a jet J with p_T . The variables \hat{s} and $\hat{\eta}$ are the partonic center-of-mass energy and parton rapidity. The SiJFs depend on the momentum fraction z_c taken by the jet, the jet energy w_J , $R' = R/\cosh(\eta)$ from the jet reconstruction algorithm, and the quark mass m_Q . The $\ln R$ resummation for jet production can be achieved by evolving the SiJFs from the jet scale μ_J to the

factorization scale μ . The renormalization group (RG) equations are the usual time-like DGLAP evolution equations. The corresponding expressions for the hard part can be found in Refs. [8, 9]. The SiJFs have been calculated up to next-to-leading order (NLO), using soft-collinear effective theory (SCET) [10–14] techniques, for light jet [15, 16] and very recently for heavy flavor jets [17]. The power corrections in proton collisions to the factorized cross section in Eq. (1.1) are of order $\Lambda_{\text{QCD}}^2/p_T^2$ and jet radius R'^2 . This factorization formula has been used to predict the inclusive and heavy flavor-tagged jet cross sections [7, 15–19]. The first application to heavy-ion collisions for light jet was given by Ref. [20]. In this paper we will extend the formalism to the case of inclusive c-jet and b-jet production in reactions with nuclei at ultra-relativistic energies. We will include all leading contributions consistent with the power counting of SCET_(M,G) [21, 22]. The medium modifications considered here are accurate up to $\mathcal{O}(\alpha_s)$ in QCD, to first order in the opacity of nuclear matter, and $\mathcal{O}(\mu^2/p_T^2)$ in SCET_(M,G) where μ is the Debye screening mass.

In heavy-ion collisions, one expects the formation of a new deconfined state of matter, known as the quark-gluon plasma (QGP). Energetic parton propagation and shower formation in this strongly interacting matter alter light particle, heavy flavor, and jet observables in heavy-ion relative to proton collisions - a phenomenon known as the jet quenching effect. Studies of jet quenching, especially for the heavy flavor-tagged jets, can reveal the fundamental thermodynamic and transport properties of the QGP. For an experimental perspective on this issue see [23] and references therein. It is well-understood that the jet quenching effects depend on the flavor of the fragmenting parton which, together with heavy quark mass effects, can be studied by light jet and heavy flavor tagged jet (c-jet and b-jet) observables in heavy ion collisions. Mass effects are expected to play a significant role in the small and intermediate transverse momentum regions and are, of course, most pronounced for b-jets [24–26]. They can also change the relative importance of radiative and collisional processes in the QGP for the modification of jet cross sections and jet substructure.

Heavy flavor studies are, therefore, central to high-energy nuclear physics since they provide new avenues to explore QCD in strongly-interacting matter and new diagnostics of its transport properties [27–29]. These efforts have been directed toward open heavy flavor, namely D-meson and B-meson production, and quarkonia. Investigation of heavy-flavor tagged jet production in heavy ion collisions has been somewhat limited thus far. Inclusive b-jets were first studied using the traditional energy loss approach [24] and later with the means of a partonic transport model [30]. Strategies to suppress the contribution from gluon splitting and enhance the fraction of prompt b-jets via energetic photon or B-meson coincident measurements opposite to the b-jet were performed in Ref. [31]. This was generalized to back-to-back b-jets [26, 32], moreover heavy flavor dijet mass distributions in heavy ion collisions were also computed [26]. The derivation of full in-medium splitting functions for light and heavy partons [22, 33, 34] allows us to bridge the gap between high energy and heavy ion theory of jet and heavy flavor production in hadronic and nuclear collisions. Their first application to b-tagged jet substructure [25] has already produced novel results, namely a unique inversion of the mass hierarchy of jet quenching effects as manifested in the stronger modification of the b-jet momentum sharing distributions in comparison to the ones for light jets. These effects are driven by the heavy quark mass

and are measurable at the LHC and by the future sPHENIX experiment at the RHIC [6]. It is, thus, important to pursue improved description of heavy flavor-tagged jet production in heavy-ion collisions using in-medium higher order calculations and resummation. On the experimental side, data in inclusive b-jet production [3] and back-to-back momentum imbalance distributions [35] exist. Measurements of c-jets in lead-lead (Pb+Pb) collisions at the LHC are expected in the near future [36].

With this in mind, in this paper we will present a calculation of the inclusive charm jet and bottom jet cross sections in heavy-ion collisions using the factorization Eq. (1.1) based on semi-inclusive fragmenting jet functions for heavy flavor. We will demonstrate that the final-state medium-induced corrections can be incorporated by modifying the SiJFs, while the short-distance hard part remains the same as p+p collisions. These corrections arise from the emergence of in-medium parton showers as the jet evolves in the QCD medium. We will study these radiative processes with the help of the medium induced splitting functions, which were calculated up to the first order in opacity in the framework of SCET with Glauber gluons (SCET_G) [21] and finite mass effects (SCET_{M,G}) [22]. The in-medium splitting functions capture the full collinear dynamics of energetic parton evolution in a QCD medium. Recent developments based on the formalism of lightcone wavefunctions [34] have allowed us to compute collinear parton branching in QCD media to any order in opacity. For the purpose of this paper, however, we will restrict ourselves to the first order in opacity results where numerical evaluation of the splitting kernels exists. Unlike the vacuum case, in the environment of strongly interacting matter jets can dissipate their energy due to collisional interactions with the medium quasi-particles. The collisional energy loss rate can be obtained, for example, from the divergence of the energy-momentum tensor of the medium induced by the color current generated by the jet [37]. This work is the first study to include this effect in the SiJF formalism. Last but not least, we also consider the cold nuclear matter (CNM) and isospin effects [38–40].

The rest of our paper is organized as follows: in Section 2 we discuss the definition of the heavy flavor jet functions in the vacuum. We derive the nuclear modifications of the jet functions in heavy-ion collisions and discuss other relevant nuclear effects. In Section 3 we present our phenomenological results for c-jet and b-jet cross sections in proton and heavy-ion collisions. Finally, we conclude in Section 4.

2 Semi-inclusive jet functions for heavy flavor

In this section, we discuss in detail the definition of the heavy quark-tagged SiJFs. For completeness, we briefly recall some analytical results from Ref. [17] for the vacuum SiJFs. We then extend these SiJFs to the case of heavy-ion collisions in the perturbative theory.

2.1 Jet Functions in vacuum

Soft-collinear effective theory can be generalized to include finite quark masses [41, 42] and is often labeled SCET_M. Within SCET_M, the heavy flavor SiJFs are obtained by calculating the real and virtual contributions inside the jet cone, and the real contributions outside the jet cone which are dependent on the jet algorithm. The NLO SiJFs for any parton to

produce a heavy flavor-tagged jet, including the heavy quark mass effects, can be found in Ref. [17]. After renormalization they are given by the following expressions

$$\begin{aligned}
J_{J_Q/Q}(z, p_T R, m, \mu) &= \delta(1-z) + \frac{\alpha_s C_F}{2\pi} \left\{ \delta(1-z) \left[f\left(\frac{m^2}{p_T^2 R^2}\right) + g\left(\frac{m^2}{p_T^2 R^2}\right) \right] \right. \\
&\quad - \left(\frac{2z}{1-z} \right)_+ \frac{m^2}{z^2 p_T^2 R^2 + m^2} + \left(\frac{1+z^2}{1-z} \right)_+ \ln \frac{\mu^2}{z^2 p_T^2 R^2 + m^2} \\
&\quad \left. - \left(2 \frac{1+z^2}{1-z} \ln(1-z) + 1-z \right)_+ \right\}, \\
J_{J_s/g}(z, p_T R, m, \mu) &= \delta(1-z) \mathcal{M}_{g \rightarrow Q\bar{Q}}^{\text{in-jet}}(p_T R, m) + \frac{\alpha_s}{2\pi} \left\{ (z^2 + (1-z)^2) \right. \\
&\quad \left. \times \ln \frac{\mu^2}{z^2(1-z)^2 p_T^2 R^2 + m^2} - 2z(1-z) \frac{z^2(1-z)^2 p_T^2 R^2}{z^2(1-z)^2 p_T^2 R^2 + m^2} \right\},
\end{aligned} \tag{2.1}$$

where the flavor singlet $J_s = J_Q + J_{\bar{Q}}$. Here, α_s is the strong coupling constant, C_F and C_A are the second Casimirs in the fundamental and adjoint representations of SU(3), respectively, m is the heavy quark mass, and R is the jet radius parameter. The function $J_{J_Q/Q}$ has both LO and NLO contributions in QCD, while $J_{J_s/g}$ starts at NLO. The functions f and g have integral representation and are defined in Ref. [17]. It was argued that, since heavy quark mass does not affect the ultraviolet (UV) behavior of diagrams, the SiJFs evolve according to DGLAP-like equations similar to the ones for light SiJFs. The RG equations read

$$\frac{d}{d \ln \mu^2} \begin{pmatrix} J_{J_Q/s}(x, \mu) \\ J_{J_s/g}(x, \mu) \end{pmatrix} = \frac{\alpha_s}{2\pi} \int_x^1 \frac{dz}{z} \begin{pmatrix} P_{qq}(z) & 2P_{gq}(z) \\ P_{qg}(z) & P_{gg}(z) \end{pmatrix} \begin{pmatrix} J_{J_Q/s}(x/z, \mu) \\ J_{J_s/g}(x/z, \mu) \end{pmatrix}. \tag{2.2}$$

Here, P_{ij} are usual Altarelli-Parisi splitting functions. The evolution equation is solved to leading logarithmic (LL) accuracy using the Mellin moment space approach developed in Ref. [43].

In the jet function $J_{J_s/g}(z, m, p_T R, \mu)$ the contribution proportional to $\delta(1-z)$ comes from the $g \rightarrow Q\bar{Q}$ splitting inside a jet. Starting only at NLO in QCD, it can be written as the integration of the jet fragmentation function $D_{Q/J_g}(z, \mu)$ ¹

$$\mathcal{M}_{g \rightarrow Q\bar{Q}}^{\text{in-jet}}(p_T R, m) = 2 \int_0^1 dz z D_{Q/J_g}(z, p_T R, m). \tag{2.3}$$

As expected, for heavy flavor a new logarithmic term $\ln p_T R/m$ arises. When $m \ll p_T R \ll p_T$, in addition to $\ln R$ the logarithmic term $\ln p_T R/m$ needs to be resummed. This can be achieved through the jet fragmentation function factorization formula found in Refs. [16, 17, 44]. In our case, up to NLO, $\mathcal{M}_{g \rightarrow Q\bar{Q}}^{\text{in-jet}}$ can be written as

$$\mathcal{M}_{g \rightarrow Q\bar{Q}}^{\text{in-jet}}(p_T R, m) = 2 \sum_{l=g, Q} \bar{K}_{l/g}(p_T R, m, \mu_F) \bar{D}_{Q/l}(m, \mu_F), \tag{2.4}$$

¹The jet fragmentation function $D_{Q/J_g}(z, \mu, m)$ is defined as the probability to find a Q quark with the momentum fraction z inside one given gluon initiated jet.

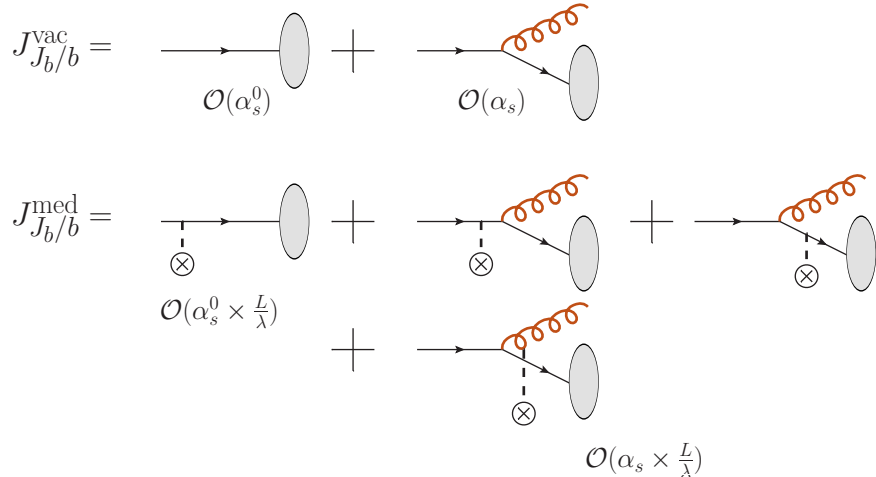


Figure 1. Illustration of real diagrams contributing to the $b \rightarrow J_b$ jet functions in perturbative QCD. The first line shows the diagrams for the LO and NLO contributions to the vacuum jet function, while the second and third lines are the corresponding medium corrections to vacuum diagrams up to the first order in opacity. The dashed lines represent the Glauber gluon exchange between the jet and the QCD medium.

where $\bar{K}_{l/g}$ is the integrated perturbative kernel at the jet typical scale $p_T R$, while $\bar{D}_{Q/l}$ is the integrated parton fragmentation function from parton l to parton Q at the scale of the quark mass. The logarithmic term $\ln p_T R/m$ can be resummed to all order at the LL accuracy by running $D_{Q/l}(m, \mu)$ from m to $p_T R$ analytically. For further details, we direct the reader to Ref. [17].

2.2 Medium corrections

In perturbative QCD, both of the LO and NLO vacuum SiJFs receive medium modifications, as illustrated in Fig. 1. For jets propagating in the forward direction, the interactions with the medium are mediated by t -channel Glauber gluon exchanges. To LO in α_s only in-medium jet energy dissipation due to collisional interactions is allowed. Such collisional energy losses have been evaluated using several different approaches in the literature [45–49]. At NLO there is vacuum radiation along with corrections from the medium-induced parton shower. In the soft gluon approximation, these would correspond to the traditional radiative energy loss in the QCD medium. In principle, one should also consider collisional energy losses along with the medium-induced parton shower. However, at present there is no theoretical formalism to derive in-medium splitting functions that simultaneously contain the energy dissipation from the t -channel Glauber gluon exchanges and properly treat the non-Abelian Landau-Pomeranchuk-Migdal effect [50]. The latter is essential to understand the cross section modification of light and heavy particles, and jets in QCD matter. Jet physics is particularly challenging, since at higher orders in α_s one needs to identify the specific partons that interact with matter, whether they contribute to the jet function or not, and their precise space-time dynamics. Branching times would enter in a model-dependent way and, since diagrams with different branching times are combined into

a medium-induced splitting kernel, even the concept of an average time for the splitting to take place is not well defined. It is at this order in α_s that the model dependence will appear. Fortunately, both collisional and radiative energy losses are small when compared to the jet transverse energy and their combined effect is suppressed relative to the individual leading contributions. We have checked numerically in the limit of long formation times for the medium-induced radiation that the combined effect can give a 10% correction at the lowest jet $p_T \sim 50$ GeV that we are interested in, and this correction disappears quickly at high p_T . For this reason, and because we want to minimize model dependence in this paper, we include the effect of collisional energy loss in the LO α_s^0 jet function for which there is no ambiguity.

We calculate in-medium branching processes to first order in opacity - an approximation that keeps quantum coherence effects between the jet production point and any one of the subsequent scattering centers in the QGP. In this framework second order in opacity will include three-body correlations, etc. It was found in the soft gluon emission limit that the first order in opacity result is a good approximation for jet quenching calculations at LHC energies [51, 52]. This is especially true for realistic plasmas of finite size and density created in heavy ion collisions and realistic geometries where a significant fraction of the jets are produced near the periphery of the interaction region and traverse thin and dilute media ². It will, of course, be important to study in the future the effects of higher orders in opacity on the full medium-induced splitting function using the method developed in Ref. [34]. These calculations are highly non-trivial, nevertheless we expect second order in opacity splitting function grids to become available in the near future [54] and to facilitate the evaluation of uncertainties arising from the opacity expansion. In this work we will calculate the medium-corrections to the NLO jet functions up to the first order in opacity which can be written as

$$J_{Q/i}^{\text{med}} = J_{Q/i}^{\text{med},(0)} + \frac{\alpha_s}{2\pi} J_{Q/i}^{\text{med},(1)}. \quad (2.5)$$

In this paper we consider for the first time the effects of jet energy dissipation through collisional interactions in the QCD medium in the fragmenting jet function formalism. We will limit our results to the LO contribution $J_{Q/i}^{\text{med},(0)}$ and defer the suppressed interplay between collisional and radiative corrections to future work. Collisional energy loss effects can be included as a transverse momentum shift of the final state jet which, to LO in perturbative QCD, is identified with the final-state hard parton. The corresponding medium modification to the cross section for the Q jet production can be written as

$$\sum_i \delta_{iQ} \left[\frac{d\sigma_{pp \rightarrow i}(p_T + \delta p_T^i, \eta)}{d(p_T + \delta p_T^i) d\eta} - \frac{d\sigma_{pp \rightarrow i}(p_T, \eta)}{dp_T d\eta} \right], \quad (2.6)$$

²Assumptions of infinite medium length and dominance of random walk processes might lead to simpler analytic results. Recent work [53], however, quantitatively and conclusively showed that an artifact of such assumptions is a gluon emission intensity that strongly underestimates the high-frequency part of the spectrum and strongly overestimates the low-frequency part of the spectrum. Numerical calculations are, thus, essential to understand in-medium parton branching.

where δ_{iQ} is the Kronecker delta symbol and δp_T^i is the average energy loss for energetic parton i moving through the hot QCD medium. As can be seen from Fig. 1, to include only the medium correction here and avoid double counting one should subtract the vacuum contribution.

We calculate collisional and radiative in-medium effects consistently in a QGP background simulated by 2+1-dimensional viscous event-by-event hydrodynamics [55]. For inclusive observables, such as the cross sections of heavy flavor-tagged jets, fluctuations do not play a role since we average over multiple hydrodynamic events. Both collisional and radiative processes in the medium arise from the same t -channel interactions between the jet and the medium. The essential information that we use is the space-time temperature profile of the QGP to evaluate the transport parameters relevant to jet quenching calculations, see Ref. [56]. For example, $\mu_D^2 = g^2 T^2 (1 + N_f/6)$ is the Debye screening scale and we use $N_f = 2$ active light quark flavors. The inverse scattering lengths of quarks and gluons are $1/\lambda_q = \sigma_{qq}\rho_q + \sigma_{qg}\rho_g$, $1/\lambda_g = \sigma_{gq}\rho_q + \sigma_{gg}\rho_g$, where ρ_q and ρ_g are the partial densities of light quarks and gluons in the QGP, respectively. The elastic scattering cross sections of fast partons on massive medium quasiparticles are given to lowest order by

$$\sigma_{qq} = \frac{1}{18\pi} \frac{g^4}{\mu_D^2}, \quad \sigma_{qg} = \frac{1}{8\pi} \frac{g^4}{\mu_D^2}, \quad \sigma_{gg} = \frac{9}{32\pi} \frac{g^4}{\mu_D^2}. \quad (2.7)$$

In Eq. (2.6), δp_T^i is obtained using collisional energy loss rate derived from an operator definition [37], where the QGP constituents are allowed to recoil³. We note that in heavy ion collisions we work with small radius jets. On the other hand, the dissipated jet energy is carried away by hydrodynamic medium excitations at angles $\mathcal{O}(1)$ relative to the direction of jet propagation [49]. Similar results were obtained in Monte-Carlo simulations of energy flow distributions inside and outside of jets in Pb+Pb collisions at the LHC [57]. Thus, we consider this energy fully lost from the point of view of jet production and the jet cross section modification can be equivalently expressed in terms of the LO in-medium jet function as

$$J_{Q/i}^{\text{med},(0)}(z, p_T, \delta p_T^i) = z \delta_{iQ} \left[\delta \left(1 - z - \frac{\delta p_T^i}{p_T + \delta p_T^i} \right) - \delta(1 - z) \right], \quad (2.8)$$

where only the diagonal part ($i = Q$) is affected by the QGP medium.

The in-medium splitting functions are expressed as integrals over the medium size and the transverse momenta transferred by the Glauber gluon [22, 33, 34]. Those integrations can only be performed numerically and we use the same QGP background [55] to obtain grids for all in-medium splitting functions to first order in opacity. The medium modification of the SiJFs can be evaluated from those grids, where a UV cut-off μ rather than the dimensional regularization scheme is used to regularize the UV poles when the transverse momentum of the vacuum radiation becomes infinity. A similar approach was employed

³In Ref. [21] we studied the effect of recoil of quasiparticles of finite mass on the cross sections for parton scattering that generates the in-medium branching processes and found this effect to be small, especially at LHC energies.

in Ref. [20] to construct the SiJFs for massless quarks and gluons. The NLO medium correction to the $Q \rightarrow J_Q$ SiJF is defined as

$$\begin{aligned}
J_{J_Q/Q}^{\text{med},(1)}(z, p_T R, m, \mu) &= \int_{z(1-z)p_{TR}}^{\mu} dq_{\perp} P_{QQ}^{\text{med}}(z, m, q_{\perp}) \\
&\quad - \delta(1-z) \int_0^1 dx \int_{x(1-x)p_{TR}}^{\mu} dq_{\perp} P_{QQ}^{\text{med}}(x, m, q_{\perp}) \\
&= \left[\int_{z(1-z)p_{TR}}^{\mu} dq_{\perp} P_{QQ}^{\text{med}}(z, m, q_{\perp}) \right]_+ .
\end{aligned} \tag{2.9}$$

In the above equation, the first line corresponds to the contribution with a radiation outside of the jet cone, while the second line represents the combination of the real radiation inside the jet cone and the virtual loop corrections. The singularity that arises when $z \rightarrow 1$ is regularized properly by the plus distribution function after combining all the corrections. The medium correction to the channel $g \rightarrow J_s = J_Q + J_{\bar{Q}}$ is

$$\begin{aligned}
J_{J_s/g}^{\text{med},(1)}(z, p_T R, m, \mu) &= \int_{z(1-z)p_{TR}}^{\mu} dq_{\perp} \left(P_{Qg}^{\text{med}}(z, m, q_{\perp}) + P_{\bar{Q}g}^{\text{med}}(z, m, q_{\perp}) \right) \\
&\quad + \delta(1-z) \int_0^1 dx \int_0^{x(1-x)p_{TR}} dq_{\perp} P_{Qg}^{\text{med}}(x, m, q_{\perp}) ,
\end{aligned} \tag{2.10}$$

where the first and second lines are the contributions with the real radiation outside and inside the jet cone, respectively.

In the application of in-medium splitting functions we use extensively sum rules. Let us take for example the momentum sum rule for the gluon initiated splitting

$$\int_0^1 x dx \left(P_{gg}(x) + \sum_i P_{ig}(x) \right) = 0 . \tag{2.11}$$

In this formulation \sum_i runs over all quark and antiquark flavors, therefore we don't have an explicit $2n_f$ factor. Since the sum rules are satisfied by the vacuum part separately, they are also satisfied by the medium-induced splitting kernels. Up to the NLO, in our previous works [15, 39] we have implemented the following normalization for the splitting functions

$$\int_0^{\mu} dq_{\perp} \int_0^1 x dx \left(P_{gg}^{\text{med}}(x) + \sum_i P_{ig}^{\text{med}}(x) \right) = 0 , \tag{2.12}$$

where the \sum_i runs over all the light flavor quarks and the q_{\perp} is the transverse momentum of the radiation. In order to keep the sum rule and consistency with our earlier calculations, for the heavy flavor splitting function we should have

$$\int_0^{\mu} dq_{\perp} \int_0^1 x dx P_{Qg}^{\text{med}}(x, q_{\perp}) = 0 \tag{2.13}$$

Using the symmetry $P_{Qg}(x, q_\perp) = P_{Qg}(1 - x, q_\perp)$ we have

$$\begin{aligned}
0 &= 2 \int_0^\mu dq_\perp \int_0^1 x dx P_{Qg}^{\text{med}}(x, q_\perp) \\
&= \int_0^\mu dq_\perp \int_0^1 x dx P_{Qg}^{\text{med}}(x, q_\perp) + \int_0^\mu dq_\perp \int_0^1 (1 - x) dx P_{Qg}^{\text{med}}(x, q_\perp) \\
&= \int_0^\mu dq_\perp dx P_{Qg}^{\text{med}}(x, q_\perp) .
\end{aligned} \tag{2.14}$$

The equation above implies that there is no additional production of open heavy flavor per nucleon-nucleon collision in heavy ion reactions. This is consistent with experimental measurements [58]. Taking this constraint into account, the function $J_{J_s/g}^{\text{med},(1)}$ becomes

$$\begin{aligned}
J_{J_s/g}^{\text{med},(1)}(z, p_T R, m, \mu) &= \left[\int_{z(1-z)p_T R}^\mu dq_\perp P_{Qg}^{\text{med}}(z, m, q_\perp) \right]_+ \\
&+ \int_{z(1-z)p_T R}^\mu dq_\perp P_{Qg}^{\text{med}}(z, m, q_\perp) .
\end{aligned} \tag{2.15}$$

The full in-medium SiJFs are defined as

$$J_{J_Q/i} = J_{J_Q/i}^{\text{vac,LL}} + J_{J_Q/i}^{\text{med}}, \tag{2.16}$$

where the vacuum contributions are calculated at the LL accuracy, while only the fixed-order medium corrections are included consistently. In this case we choose the cut-off scale μ as the jet's transverse momentum. In principle the full in-medium SiJFs obey a DGLAP-like evolution in Eq. (2.2) and one can even introduce the medium-induced splitting functions in the DGLAP kernel to fully consider the jet evolution in the QCD medium. We will leave this for a future study.

Besides final-state in-medium modifications to jet production, we have to include the initial-state ones, or CNM effects. The CNM effects arise from the coherent, elastic, and inelastic patron scattering in large nuclei only part of them can be parameterized via global nuclear PDF fits, for example nCTEQ15 PDF sets [59]. While many of these effects can be implemented as *effective* modifications of the PDFs, they are not necessarily universal. A well known example is the Cronin effect which manifests itself in the enhancement of the cross sections for particle production in proton-nucleus (p+A) reactions relative to p+p reactions at transverse momenta in the range $p_T = 1 - 5$ GeV [60]. As this enhancement range is independent of the center of mass energy of the collision, this effect does not scale with the momentum fraction of the partons in the nucleus. The most common theoretical explanation of the Cronin effect is related to the initial-state transverse momentum broadening of the partons through t -channel interactions with cold nuclear matter [61–63]. As we have seen in the case of the QGP, these interactions will lead to medium-induced radiation. Its spectrum was first computed for beam jets by Bertsch and Gunion [64] to provide a perturbative explanation of the nearly flat rapidity distribution of soft particles produced in hadronic collisions. Naturally, in p+A collisions the radiation intensity will be amplified and, as hard partons lose a small fraction of their energy, the cross sections for particle and

jet production can be reduced. The first measurement to support this energy loss picture was performed at a Fermilab fixed target experiment [65] for J/ψ s, where the strong suppression of the cross section was found to scale with the momentum fraction of the parton from the proton and not with the momentum fraction of the parton from the nucleus. This shows conclusively that the effect does not arise from nuclear PDF modification, but is in line with the expectations from the picture of parton energy loss in large nuclei [66, 67]. The same scaling and physical picture were later confirmed at collider energies [68, 69].

Most recently, measurements of jets at RIHC and LHC in deuterium-gold (d+Au) and proton-lead (p+Pb), respectively, have also revealed cross suppression in central and semi-central collisions [70, 71]. This experimentally determined modification of the jet cross sections was also found to scale with a variable proportional to the momentum fraction of the parton in the proton and evaluated in a picture of parton energy loss in cold nuclear matter [38]. The radiation from the beam jets was numerically calculated as in Ref. [72] and is implemented as a shifts in Bjorken x variable in the PDFs as follows:

$$f_{q/A}(x, \mu) \rightarrow f_{q/A}\left(\frac{x}{1 - \epsilon_q}, \mu\right), \quad f_{g/A}(x, \mu) \rightarrow f_{g/A}\left(\frac{x}{1 - \epsilon_g}, \mu\right). \quad (2.17)$$

This shift is related to the energy fraction $\epsilon_{q,g}$ that the parton loses in cold nuclear matter and depends on the parton flavor. The cross section suppression effect will be the largest for large values of Bjorken x because of the steeply falling parton distributions as a function of x . One example that we have studied besides jets is the attenuation of di-muons in fixed target Drell-Yan production [73]. For the smaller jet p_T ranges that we consider here relative to the ATLAS p+Pb measurement [70] the effect will be reduced, as we move away from the kinematic bounds. However, in nucleus-nucleus (A+A) collisions it will be amplified since partons from both nuclei pass through the opposite going nucleus. In this calculation we also have control over the centrality dependence of the CNM effects, for example they are $\sim 20\%$ bigger per nucleus in central relative to minimum bias Pb+Pb collisions. For the case of nuclei, we include with relevant weights Z and $A - Z$ the proton and neutron PDFs, respectively, where the latter are constructed from the proton PDFs using isospin symmetry. The validation of our evaluation of CNM effects will be discussed in Fig. 4 by comparing the predicted R_{pA} to CMS measurements.

3 Numerical results

In this section we present our numerical predictions for inclusive c-jet and b-jet production in hadronic collisions. For our work we choose the CT14NLO PDF sets [74]. The hard part in the factorized cross section is calculated at NLO with massless b- and c-quarks, while the mass effect is included in the c- and b-jet SiJFs. The UV cut-off and the scale of α_s in the medium corrections to the jet functions are set to be the factorization scale μ . The default factorization and jet scales are chosen to be $\mu = p_T$ and $\mu_J = p_T R$, respectively. The uncertainties are evaluated by varying μ and μ_J by a factor of 2 independently. The

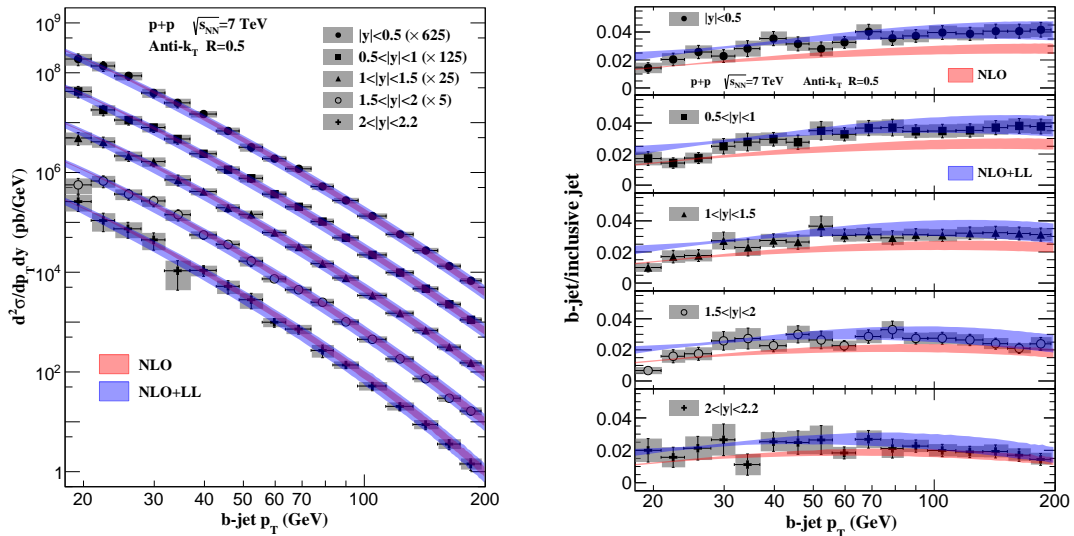


Figure 2. Comparison of theoretical predictions and measurements for b-jets with radius $R = 0.5$ in p+p collisions at $\sqrt{s_{\text{NN}}} = 7$ TeV. The b-jet cross section (left) and the ratio of the b-jet cross section to the inclusive jet cross section (right) are shown as a function of jet p_T for different rapidity intervals. The red and blue bands are the NLO and NLO+LL predictions, respectively, while the gray bars represent the total experimental uncertainty of the data [2].

coupling between the jet and the medium, which appears in the modification to the SiJFs, is set as $g = 2$ ⁴.

Before we move on to jet production in heavy-ion collisions, we must address inclusive b-jet and c-jet production in p+p collisions. These cross sections set the baseline relative to which cross section modifications with nuclei can be detected. Figure 2 presents the comparison between our theoretical results for the inclusive b-jet cross section (left) and the fraction of b-jets to inclusive light jets (right) for different rapidity intervals as a function of the jet transverse momentum p_T . The colliding system is p+p with $\sqrt{s_{\text{NN}}} = 7$ TeV and jet reconstruction parameter $R = 0.5$. The $\ln R$ resummed cross sections for b-jet changes the NLO predictions by $\mathcal{O}(10\%)$, but we find larger scale uncertainties. The NLO and NLO+LL p_T distributions presented here are consistent with the predictions from Ref. [17] and the experimental measurements [2]. For the b-jet fraction, the difference between NLO+LL and NLO visible in the right panel of Figure 2 can be traced also to the differences in the inclusive jet cross section. The $\ln R$ resummation reduces the inclusive jet cross more significantly. The NLO+LL predictions agree very well with the data.

We now move on to c-jets and their cross sections in p+p collisions are shown in Fig. 3 for center-of-mass energies 5.02 TeV (left) and 2.76 TeV (right), respectively. Similar to b-jet cross section, the $\ln R$ resummation changes the c-jet cross section by about 10% in a p_T -dependent fashion, but with larger theoretical uncertainties. We also note that in

⁴ The average strong coupling constant is $\bar{\alpha}_s = g^2/4\pi = 0.32$ consistent with many other studies on jet quenching effects [20, 24–26, 39, 75]. Comparison between predictions based on the medium-induced splitting functions and data might provide a way to extract the coupling $\bar{\alpha}_s$, though one should be mindful of theoretical model uncertainties.

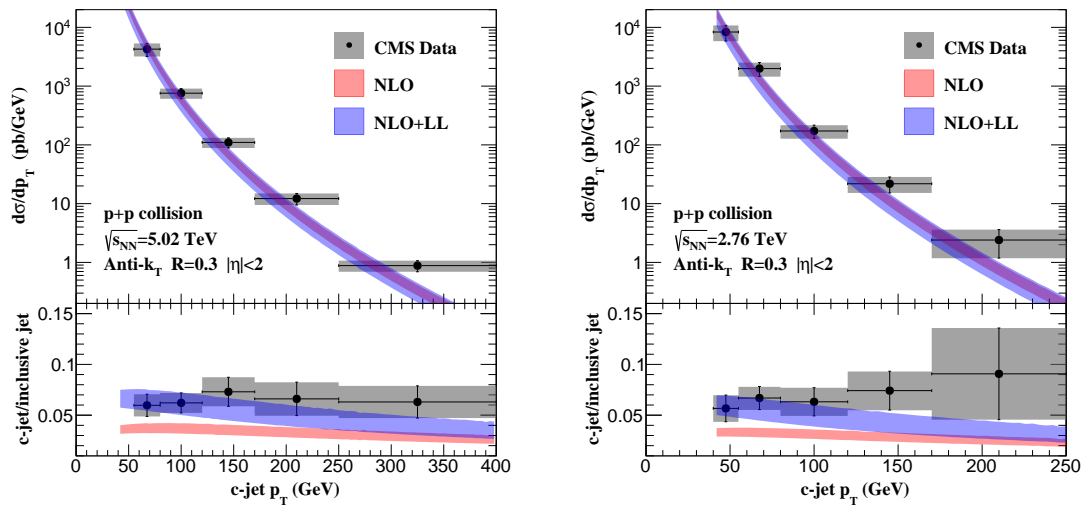


Figure 3. The c-jet cross sections (top) and their ratios (bottom) to the inclusive jet cross sections as a function of jet p_T in p+p collisions at $\sqrt{s_{NN}} = 5.02$ TeV (left) and 2.76 TeV (right). The jets are reconstructed using the anti- k_T algorithm with $R=0.3$ and the pseudorapidity cut $|\eta| < 2$ is imposed. The color scheme is the same as in Fig. 2.

comparison to b-jets the spectrum appears stiffer, and our calculation agrees better with the experimental measurements at lower p_T . This is also reflected in the right panel of Fig. 3. Again, the NLO+LL c-jet fractions agree better with CMS measurements [5] when compared to the NLO ones for both collision energies.

The high energy jet production in proton-nucleus collisions can place constraints on the CNM effects. Early ATLAS and PHENIX measurements suggested that the suppression of inclusive jet cross sections, especially at high p_T and in central p+Pb collisions⁵, can be large [70, 71]. The ALICE collaboration as further studied the event activity in semi-inclusive hadron-jet distributions [76]. In minimum bias collisions, the modification of jet cross sections, if any, is smaller. Within the statistical and systematic uncertainties many measurements are consistent with a range of possibilities - from no nuclear effects to $\pm 10\%$ cross section modification. The way in which the modification due to in-medium QCD effects is experimentally and theoretically studied is through the ratio

$$R_{AB} = \frac{1}{\langle N_{bin}^{AB} \rangle} \frac{d\sigma^{AB}/d(PS)}{d\sigma^{pp}/d(PS)}. \quad (3.1)$$

Here, $\langle N_{bin}^{AB} \rangle$ is the average number of binary collisions between proton/nucleus A and proton/nucleus B and $d(PS)$ is the relevant phase space differential - in our case in the jet transverse momentum p_T . An added advantage of the observable defined in Eq. (3.1) is that uncertainties in the absolute normalization of the cross section largely cancel in the ratio.

We can use proton-lead collisions at the LHC to check the validity of our theoretical model. At the high jet transverse momenta under investigation, we take into account the

⁵Determination of centrality in p+A collisions can be subtle, thereby influencing the experimentally measured nuclear modification.

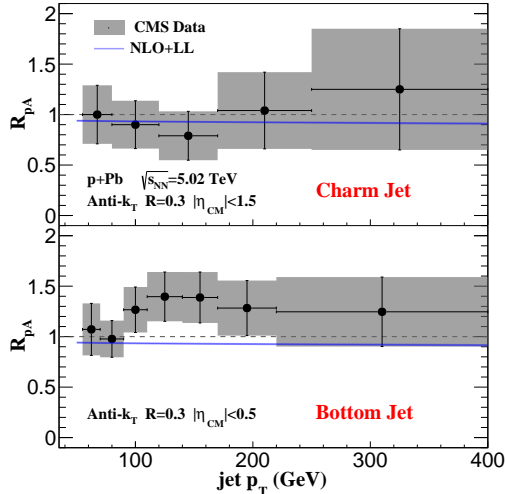


Figure 4. Comparison of theoretical predictions for the heavy flavor jet cross sections in proton-nucleus collisions R_{pA} to CMS measurements [4, 5] of c-jets (top) and b-jets (bottom). The system is p+Pb at $\sqrt{s_{NN}} = 5.02$ TeV and the jets are constructed using the anti- k_T algorithm with $R = 0.3$. The rapidity cut in the center-of-mass frame is $|\eta_{CM}| < 1.5$ for c-jets and $|\eta_{CM}| < 0.5$ for b-jets.

initial-state CNM energy loss [38]. In Fig. 4, we compare our calculated nuclear modification factor R_{pA} for heavy flavor tagged-jets to the CMS experimental measurements [4, 5] in 5.02 TeV p+Pb collisions. The scale dependence of the cross sections in p+Pb collisions is almost the same as the one in p+p collisions. Therefore, the NLO+LL ratio R_{pA} changes very little with scale variation. Furthermore there is not an obvious difference between the predicted c-jet and b-jet R_{pA} , which is between 0.9 and 0.95 for the jet transverse momentum in the range of $50 \text{ GeV} < p_T < 400 \text{ GeV}$. The NLO+LL jet cross section modification R_{pA} for c-jet, displayed in the top panel, describes the CMS data [5] very well. In the bottom panel, the prediction is on the lower edge of the experimental error bar [4] and cannot describe the fluctuation of the data around $p_T \sim 150 \text{ GeV}$. Given experimental uncertainties, however, there is no significant deviation between predictions and the measurements. It is worth noticing that in Pb+Pb collisions CNM effects will be amplified when compared to p+Pb collisions because there is one more nucleus in the initial state.

To proceed to nucleus-nucleus reactions, we include final-state interactions. In Fig. 5 we show the theoretical model predictions for the in-medium suppression factor R_{AA} for b-jets with $|\eta| < 2$, reconstructed with the anti- k_T algorithm with $R=0.3$ at $\sqrt{s_{NN}}=5.02$ TeV. The effect of the medium-induced parton shower is represented by the green band. Compared to the light jet results from Ref. [20], the effect of in-medium radiative processes on b-jets is noticeably smaller. The reason for that lies in the strength of the medium-induced parton shower contribution to b-jet production, which is predominantly proportional to the second Casimir in the color representation of the parent parton and is smaller for quark-initiated jets. The difference between the blue and green bands in Fig. 5 represents the jet energy dissipation in the medium due to collisional processes. It is of the same order as the medium-

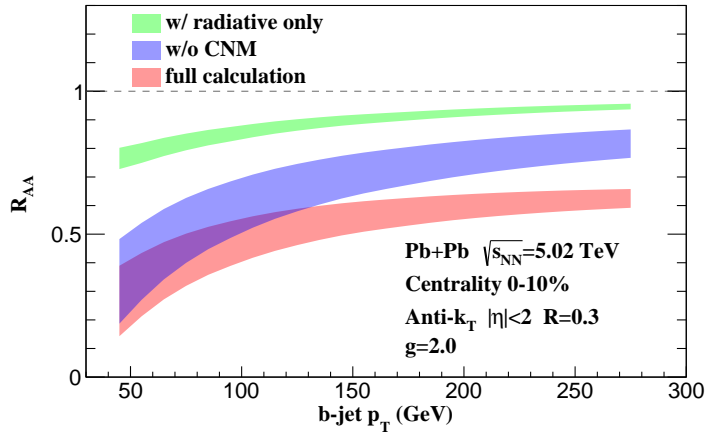


Figure 5. The b-jet suppression factor for central Pb+Pb collision at $\sqrt{s_{NN}}=5.02$ TeV, where anti- k_T algorithm with $R=0.3$ and jet $|\eta| < 2$ are implemented. The R_{AA} with all nuclear effects included is shown as the red band. The blue band presents the prediction without the CNM effects, while the green band corresponds to the result with only in-medium radiative processes included.

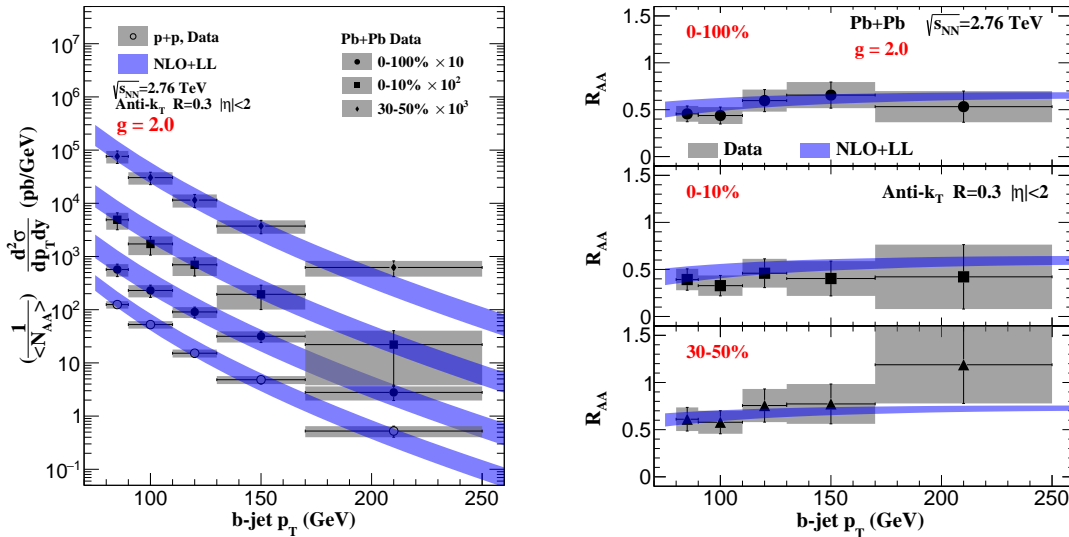


Figure 6. The b-jet cross sections (left) in p+p and Pb+Pb collisions and the nuclear modification factor R_{AA} (right) for different centrality classes (0-100%, 0-10% and 30-50%), as indicated in the legend. All theoretical predictions are present as the blue bands and are compared to the data from CMS measurements [3].

induced out-of cone radiation and is more important when the jet transverse momentum is small. The CNM effects, represented by the difference between the blue and red bands, are more important in the high energy regime, especially when the attenuation due to final-state effects become smaller. As expected, they are more than twice larger than the R_{pA} in Fig. 4 since we consider central Pb+Pb collisions. The full nuclear modification factor R_{AA} is about 0.3 for $p_T \sim 50$ GeV and about 0.6 for $p_T \sim 250$ GeV. Even though the b-jet R_{AA} is found to be qualitatively consistent with that of inclusive jets from measurements with the same collision energy [77, 78], the underlying physics might be different.

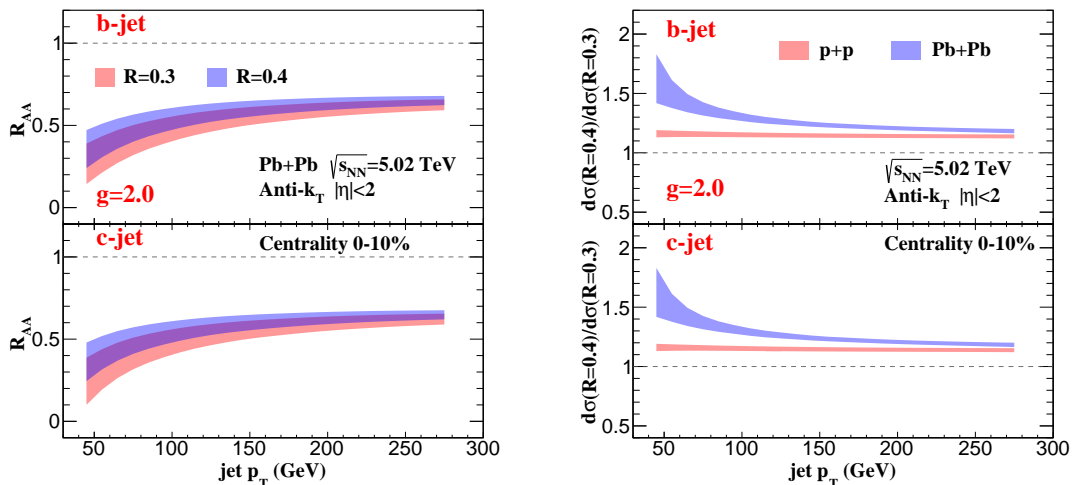


Figure 7. The heavy flavor tagged jet nuclear suppression factor R_{AA} (left) and the cross section ratio for different radii (right). In the left plot, the red and blue bands represent the R_{AA} for $R=0.3$ and 0.4 , respectively. The cross section ratio is defined as $\frac{d\sigma(R=0.4)}{dp_T} / \frac{d\sigma(R=0.3)}{dp_T}$ with the red and blue bands for p+p and Pb+Pb collisions, respectively. The upper panels present our results for b-jet and the lower ones for c-jet.

In Fig. 6 we compare our numerical calculations to the measurements [3] of b-jet production in p+p and Pb+Pb collisions with $\sqrt{s_{NN}} = 2.76$ TeV. The left plot shows the inclusive b-jet p_T distributions, where the cross sections in heavy-ion collisions with centrality 0-100%, 0-10% and 30-50% are scaled by powers of 10 for visibility. The right plot presents the nuclear modification factor R_{AA} with the same settings. In general R_{AA} decreases (larger suppression) with increasing collision centrality (toward head-on nuclear collisions). From the data, the attenuation factor R_{AA} seems less dependent on the centrality when compared to the well-known light jet modification. The predictions agree very well with the data for both the inclusive cross sections and the nuclear modification factors. QCD medium corrections depend on the center-of-mass energy, colliding nuclei, and the centrality of the collision itself. Thus, the agreement between data and theory seen in Fig. 6 is already a non-trivial test of the predictive power of the semi-inclusive jet function formalism in QCD matter. As we pointed out early on, first predictions for heavy flavor jet substructure using the same in-medium splitting functions have been presented by us [25]. Future measurements of this observable at the LHC and by the sPHENIX experiment at RHIC can further test the universality of the medium induced corrections to b-jets and c-jets.

Figure 7 presents our predictions for the suppression R_{AA} of c-jets and b-jets (left) and the cross section ratio for different jet radii (right) as a function of jet p_T at $\sqrt{s_{NN}} = 5.02$ TeV. Since the CNM effects and collisional energy loss do not depend on the jet radius for small R , consequently, the radius dependence of R_{AA} is reduced relative to the case where only in-medium radiative processes contribute. For example, in the earlier study of inclusive light jet modification [20] collisional energy losses were not included and, consequently, the

calculated radius dependence was larger. In p+p collisions, the ratio of the cross section with $R = 0.4$ to that with $R = 0.3$ practically does not depend on jet p_T . On the other hand, there is small dependence on jet p_T in Pb+Pb collisions. It can be seen from Fig. 7 that the smaller radius jet tends to dissipate more energy in the medium. There is no significant difference between the c-jet and b-jet due to the high transverse momentum where heavy quark mass effects are small to negligible. In the small transverse momentum region where the uncertainty of our calculations is relatively large, the contribution from higher orders in opacity [34] might play an important role. which can be included either by calculating higher order splitting functions [79] or by solving the RG equation with the medium-corrected DGLAP kernel [39]. This can be one of the interesting applications of this framework in the future.

4 Conclusions

In this work, we presented a formalism to study heavy flavor jet production in hadronic *and* heavy-ion collisions using the heavy flavor semi-inclusive jet functions. This approach relies on hard-collinear factorization, where the cross section is expressed as the convolution of the PDFs, the hard kernel, and jet functions. For light-flavor jets, similar formalism has been applied to the inclusive jet production and jet substructure yielding gains in the accuracy of theoretical predictions. It has also helped place jet calculations in heavy ion collisions on the firmer theoretical ground. With this in mind, we presented the first calculation of heavy flavor jets in heavy ion collisions using the heavy flavor semi-inclusive jet functions technique. For jets produced in hadronic collisions, the important $\ln R$ terms were resummed up to leading logarithmic accuracy using a DGLAP-like evolution of the vacuum jet fragmenting functions. In heavy ion collisions the medium corrections are included consistently up to next-to-leading order in QCD and first order in opacity. This limits the applicability of our approach at small jet transverse momenta, where such medium corrections can become large and need to also be numerically resummed. We defer this study to future work.

We compared the theoretical cross section results for inclusive c-jet and b-jet production to the experimental data from p+p and Pb+Pb collisions and found very good agreement between data from the Large Hadron Collider and theory. For the more complex heavy ion collisions, we did include the CNM effects and, for the first time, collisional energy losses in the jet fragmentation function formalism. These were shown to play an important role in the overall suppression of the heavy flavor jet cross sections. We further presented our calculations of c-jet and b-jet cross sections and their modification R_{pA} in the cold nuclear matter. Comparison to data at $\sqrt{s_{NN}} = 5.02$ TeV demonstrates that, while experimental error bars are large, the CNM effects employed in this calculation are compatible with measurement. We finally showed the predictions of R_{AA} for the production and attenuation of c-jets and b-jets of different radii in the highest center-of-mass energy Pb+Pb collisions. With such developments in place, it might be useful to revisit the calculation of photon-tagged heavy flavor jets [31] and back-to-back b-jets [26], which so far have only been considered in the soft gluon approximation medium-induced energy loss limit.

In future, we plan to further investigate heavy flavor-tagged jet substructure observables. Energy correlators inside jets [80] are being evaluated in the framework of SCET [81]. It would be interesting to calculate them in heavy ion collisions, and for such observables inclusion of higher orders-in-opacity corrections in the medium [34] might be important. We further expect that resummation if the in-medium branchings will improve the predictions in the small- p_T region, allowing access to the kinematic domain where mass effects on the heavy flavor jet production and propagation in a dense QCD are most pronounced and can lead to novel phenomena [25]. With a proper extension, we expect that this formalism will be well-suited to investigate jet shapes in hadronic [82–84] and heavy ion collisions [75]. Other observables of interest are collinear [85] and transverse momentum fragmentation functions [86, 87] for a hadron production inside jets, extended to heavy flavor⁶. The application of the extended formalism to such observables will provide an important test of the universality of the medium modifications predicted by the SCET_(M,G) framework. We finally remark that our approach is also applicable to heavy flavor jet production at a future electron-ion collider.

Acknowledgements

We would like to thank Zhong-Bo Kang, Emanuele Mereghetti and Felix Ringer for useful discussions. This work was supported by the U.S. Department of Energy under Contract No. DE-AC52-06NA25396, its Early Career Program, and the Los Alamos National Laboratory LDRD program.

References

- [1] G. F. Sterman and S. Weinberg, *Jets from Quantum Chromodynamics*, *Phys. Rev. Lett.* **39** (1977) 1436.
- [2] CMS collaboration, S. Chatrchyan et al., *Inclusive b-jet production in pp collisions at $\sqrt{s} = 7$ TeV*, *JHEP* **04** (2012) 084, [[1202.4617](#)].
- [3] CMS collaboration, S. Chatrchyan et al., *Evidence of b-Jet Quenching in PbPb Collisions at $\sqrt{s_{NN}} = 2.76$ TeV*, *Phys. Rev. Lett.* **113** (2014) 132301, [[1312.4198](#)].
- [4] CMS collaboration, V. Khachatryan et al., *Transverse momentum spectra of inclusive b jets in pPb collisions at $\sqrt{s_{NN}} = 5.02$ TeV*, *Phys. Lett.* **B754** (2016) 59, [[1510.03373](#)].
- [5] CMS collaboration, A. M. Sirunyan et al., *Measurements of the charm jet cross section and nuclear modification factor in pPb collisions at $\sqrt{s_{NN}} = 5.02$ TeV*, *Phys. Lett.* **B772** (2017) 306–329, [[1612.08972](#)].
- [6] PHENIX collaboration, A. Adare et al., *An Upgrade Proposal from the PHENIX Collaboration*, [1501.06197](#).
- [7] T. Kaufmann, A. Mukherjee and W. Vogelsang, *Hadron Fragmentation Inside Jets in Hadronic Collisions*, *Phys. Rev.* **D92** (2015) 054015, [[1506.01415](#)].

⁶Note that in Ref. [88] D^* production inside jets was used to constrain fragmentation into open heavy flavor, but the analysis relied on semi-inclusive fragmenting jet functions for massless partons.

- [8] F. Aversa, P. Chiappetta, M. Greco and J. P. Guillet, *QCD Corrections to Parton-Parton Scattering Processes*, *Nucl. Phys.* **B327** (1989) 105.
- [9] B. Jager, A. Schafer, M. Stratmann and W. Vogelsang, *Next-to-leading order QCD corrections to high p_T pion production in longitudinally polarized pp collisions*, *Phys. Rev.* **D67** (2003) 054005, [[hep-ph/0211007](#)].
- [10] C. W. Bauer, S. Fleming and M. E. Luke, *Summing Sudakov logarithms in $B \rightarrow X_s + \gamma$ in effective field theory*, *Phys. Rev.* **D63** (2000) 014006, [[hep-ph/0005275](#)].
- [11] C. W. Bauer, S. Fleming, D. Pirjol and I. W. Stewart, *An Effective field theory for collinear and soft gluons: Heavy to light decays*, *Phys. Rev.* **D63** (2001) 114020, [[hep-ph/0011336](#)].
- [12] C. W. Bauer and I. W. Stewart, *Invariant operators in collinear effective theory*, *Phys. Lett.* **B516** (2001) 134–142, [[hep-ph/0107001](#)].
- [13] C. W. Bauer, D. Pirjol and I. W. Stewart, *Soft collinear factorization in effective field theory*, *Phys. Rev.* **D65** (2002) 054022, [[hep-ph/0109045](#)].
- [14] M. Beneke, A. P. Chapovsky, M. Diehl and T. Feldmann, *Soft collinear effective theory and heavy to light currents beyond leading power*, *Nucl. Phys.* **B643** (2002) 431–476, [[hep-ph/0206152](#)].
- [15] Z.-B. Kang, F. Ringer and I. Vitev, *The semi-inclusive jet function in SCET and small radius resummation for inclusive jet production*, *JHEP* **10** (2016) 125, [[1606.06732](#)].
- [16] L. Dai, C. Kim and A. K. Leibovich, *Fragmentation of a Jet with Small Radius*, *Phys. Rev.* **D94** (2016) 114023, [[1606.07411](#)].
- [17] L. Dai, C. Kim and A. K. Leibovich, *Heavy Quark Jet Fragmentation*, *JHEP* **09** (2018) 109, [[1805.06014](#)].
- [18] M. Dasgupta, F. Dreyer, G. P. Salam and G. Soyez, *Small-radius jets to all orders in QCD*, *JHEP* **04** (2015) 039, [[1411.5182](#)].
- [19] M. Dasgupta, F. A. Dreyer, G. P. Salam and G. Soyez, *Inclusive jet spectrum for small-radius jets*, *JHEP* **06** (2016) 057, [[1602.01110](#)].
- [20] Z.-B. Kang, F. Ringer and I. Vitev, *Inclusive production of small radius jets in heavy-ion collisions*, *Phys. Lett.* **B769** (2017) 242–248, [[1701.05839](#)].
- [21] G. Ovanessian and I. Vitev, *An effective theory for jet propagation in dense QCD matter: jet broadening and medium-induced bremsstrahlung*, *JHEP* **06** (2011) 080, [[1103.1074](#)].
- [22] Z.-B. Kang, F. Ringer and I. Vitev, *Effective field theory approach to open heavy flavor production in heavy-ion collisions*, *JHEP* **03** (2017) 146, [[1610.02043](#)].
- [23] M. Connors, C. Nattrass, R. Reed and S. Salur, *Jet measurements in heavy ion physics*, *Rev. Mod. Phys.* **90** (2018) 025005, [[1705.01974](#)].
- [24] J. Huang, Z.-B. Kang and I. Vitev, *Inclusive b -jet production in heavy ion collisions at the LHC*, *Phys. Lett.* **B726** (2013) 251–256, [[1306.0909](#)].
- [25] H. T. Li and I. Vitev, *Inverting the mass hierarchy of jet quenching effects with prompt b -jet substructure*, *Phys. Lett.* **B793** (2019) 259–264, [[1801.00008](#)].
- [26] Z.-B. Kang, J. Reiten, I. Vitev and B. Yoon, *Light and heavy flavor dijet production and dijet mass modification in heavy ion collisions*, *Phys. Rev.* **D99** (2019) 034006, [[1810.10007](#)].

- [27] A. Andronic et al., *Heavy-flavour and quarkonium production in the LHC era: from proton-proton to heavy-ion collisions*, *Eur. Phys. J.* **C76** (2016) 107, [[1506.03981](#)].
- [28] A. Beraudo et al., *Extraction of Heavy-Flavor Transport Coefficients in QCD Matter*, *Nucl. Phys.* **A979** (2018) 21–86, [[1803.03824](#)].
- [29] S. Cao et al., *Toward the determination of heavy-quark transport coefficients in quark-gluon plasma*, *Phys. Rev.* **C99** (2019) 054907, [[1809.07894](#)].
- [30] F. Senzel, J. Uphoff, Z. Xu and C. Greiner, *The different energy loss mechanisms of inclusive and b-tagged reconstructed jets within ultra-relativistic heavy-ion collisions*, *Phys. Lett.* **B773** (2017) 620–624, [[1602.05086](#)].
- [31] J. Huang, Z.-B. Kang, I. Vitev and H. Xing, *Photon-tagged and B-meson-tagged b-jet production at the LHC*, *Phys. Lett.* **B750** (2015) 287–293, [[1505.03517](#)].
- [32] W. Dai, S. Wang, S.-L. Zhang, B.-W. Zhang and E. Wang, *Transverse Momentum Balance and Angular Distribution of $b\bar{b}$ Dijets in Pb+Pb collisions*, [1806.06332](#).
- [33] G. Ovanessian and I. Vitev, *Medium-induced parton splitting kernels from Soft Collinear Effective Theory with Glauber gluons*, *Phys. Lett.* **B706** (2012) 371–378, [[1109.5619](#)].
- [34] M. D. Sievert and I. Vitev, *Quark branching in QCD matter to any order in opacity beyond the soft gluon emission limit*, *Phys. Rev.* **D98** (2018) 094010, [[1807.03799](#)].
- [35] CMS collaboration, A. M. Sirunyan et al., *Comparing transverse momentum balance of b jet pairs in pp and PbPb collisions at $\sqrt{s_{NN}} = 5.02$ TeV*, *JHEP* **03** (2018) 181, [[1802.00707](#)].
- [36] H. Hassan, *Charm jet production and properties in pp, p-Pb, and PbPb collisions measured with ALICE at the LHC*, in *19th International Workshop on Charm Physics (CHARM 2018)*, (Novosibirsk, Russia), May, 2018.
- [37] R. B. Neufeld, I. Vitev and H. Xing, *Operator definition and derivation of collisional energy and momentum loss in relativistic plasmas*, *Phys. Rev.* **D89** (2014) 096003, [[1401.5101](#)].
- [38] Z.-B. Kang, I. Vitev and H. Xing, *Effects of cold nuclear matter energy loss on inclusive jet production in p+A collisions at energies available at the BNL Relativistic Heavy Ion Collider and the CERN Large Hadron Collider*, *Phys. Rev.* **C92** (2015) 054911, [[1507.05987](#)].
- [39] Y.-T. Chien, A. Emerman, Z.-B. Kang, G. Ovanessian and I. Vitev, *Jet Quenching from QCD Evolution*, *Phys. Rev.* **D93** (2016) 074030, [[1509.02936](#)].
- [40] J. L. Albacete et al., *Predictions for Cold Nuclear Matter Effects in p+Pb Collisions at $\sqrt{s_{NN}} = 8.16$ TeV*, *Nucl. Phys.* **A972** (2018) 18–85, [[1707.09973](#)].
- [41] I. Z. Rothstein, *Factorization, power corrections, and the pion form-factor*, *Phys. Rev.* **D70** (2004) 054024, [[hep-ph/0301240](#)].
- [42] A. K. Leibovich, Z. Ligeti and M. B. Wise, *Comment on quark masses in SCET*, *Phys. Lett.* **B564** (2003) 231–234, [[hep-ph/0303099](#)].
- [43] A. Vogt, *Efficient evolution of unpolarized and polarized parton distributions with QCD-PEGASUS*, *Comput. Phys. Commun.* **170** (2005) 65–92, [[hep-ph/0408244](#)].
- [44] C. W. Bauer and E. Mereghetti, *Heavy Quark Fragmenting Jet Functions*, *JHEP* **04** (2014) 051, [[1312.5605](#)].
- [45] J. D. Bjorken, *Energy Loss of Energetic Partons in Quark-Gluon Plasma: Possible Extinction of High p(t) Jets in Hadron-Hadron Collisions*, .

- [46] E. Braaten and M. H. Thoma, *Energy loss of a heavy quark in the quark - gluon plasma*, *Phys. Rev.* **D44** (1991) R2625.
- [47] S. Wicks, W. Horowitz, M. Djordjevic and M. Gyulassy, *Elastic, inelastic, and path length fluctuations in jet tomography*, *Nucl. Phys.* **A784** (2007) 426–442, [[nucl-th/0512076](#)].
- [48] P. B. Gossiaux and J. Aichelin, *Towards an understanding of the RHIC single electron data*, *Phys. Rev.* **C78** (2008) 014904, [[0802.2525](#)].
- [49] R. B. Neufeld and I. Vitev, *Parton showers as sources of energy-momentum deposition in the QGP and their implication for shockwave formation at RHIC and at the LHC*, *Phys. Rev.* **C86** (2012) 024905, [[1105.2067](#)].
- [50] X.-N. Wang, M. Gyulassy and M. Plumer, *The LPM effect in QCD and radiative energy loss in a quark gluon plasma*, *Phys. Rev.* **D51** (1995) 3436–3446, [[hep-ph/9408344](#)].
- [51] M. Gyulassy, P. Levai and I. Vitev, *NonAbelian energy loss at finite opacity*, *Phys. Rev. Lett.* **85** (2000) 5535–5538, [[nucl-th/0005032](#)].
- [52] M. Gyulassy, P. Levai and I. Vitev, *Reaction operator approach to nonAbelian energy loss*, *Nucl. Phys.* **B594** (2001) 371–419, [[nucl-th/0006010](#)].
- [53] X. Feal and R. Vazquez, *Intensity of gluon bremsstrahlung in a finite plasma*, *Phys. Rev.* **D98** (2018) 074029, [[1811.01591](#)].
- [54] M. D. Sievert, I. Vitev and B. Yoon, *A complete set of in-medium splitting functions to any order in opacity*, [1903.06170](#).
- [55] C. Shen, Z. Qiu, H. Song, J. Bernhard, S. Bass and U. Heinz, *The iEBE-VISHNU code package for relativistic heavy-ion collisions*, *Comput. Phys. Commun.* **199** (2016) 61–85, [[1409.8164](#)].
- [56] S. Aronson, E. Borrás, B. Odegard, R. Sharma and I. Vitev, *Collisional and thermal dissociation of J/ψ and Υ states at the LHC*, *Phys. Lett.* **B778** (2018) 384–391, [[1709.02372](#)].
- [57] Y. Tachibana, N.-B. Chang and G.-Y. Qin, *Full jet in quark-gluon plasma with hydrodynamic medium response*, *Phys. Rev.* **C95** (2017) 044909, [[1701.07951](#)].
- [58] PHENIX collaboration, K. Adcox et al., *Measurement of single electrons and implications for charm production in Au+Au collisions at $\sqrt{s_{NN}} = 130$ GeV*, *Phys. Rev. Lett.* **88** (2002) 192303, [[nucl-ex/0202002](#)].
- [59] K. Kovarik et al., *nCTEQ15 - Global analysis of nuclear parton distributions with uncertainties in the CTEQ framework*, *Phys. Rev.* **D93** (2016) 085037, [[1509.00792](#)].
- [60] J. W. Cronin, H. J. Frisch, M. J. Shochet, J. P. Boymond, R. Mermod, P. A. Piroué et al., *Production of hadrons with large transverse momentum at 200, 300, and 400 GeV*, *Phys. Rev.* **D11** (1975) 3105–3123.
- [61] Y. Zhang, G. I. Fai, G. Papp, G. G. Barnafoldi and P. Levai, *High p_T pion and kaon production in relativistic nuclear collisions*, *Phys. Rev.* **C65** (2002) 034903, [[hep-ph/0109233](#)].
- [62] A. Accardi and D. Treleani, *Minijet transverse spectrum in high-energy hadron nucleus collisions*, *Phys. Rev.* **D64** (2001) 116004, [[hep-ph/0106306](#)].
- [63] I. Vitev and M. Gyulassy, *High p_T tomography of $d + Au$ and $Au+Au$ at SPS, RHIC, and LHC*, *Phys. Rev. Lett.* **89** (2002) 252301, [[hep-ph/0209161](#)].

- [64] J. F. Gunion and G. Bertsch, *Hadronization by color bremsstrahlung*, *Phys. Rev.* **D25** (1982) 746.
- [65] NUSEA collaboration, M. J. Leitch et al., *Measurement of J/ψ and ψ' suppression in p - A collisions at 800-GeV/c*, *Phys. Rev. Lett.* **84** (2000) 3256–3260, [[nucl-ex/9909007](#)].
- [66] S. Gavin and J. Milana, *Energy loss at large $x(F)$ in nuclear collisions*, *Phys. Rev. Lett.* **68** (1992) 1834–1837.
- [67] R. Vogt, *The $x(F)$ dependence of ψ and Drell-Yan production*, *Phys. Rev.* **C61** (2000) 035203, [[hep-ph/9907317](#)].
- [68] PHENIX collaboration, S. S. Adler et al., *J/ψ production and nuclear effects for $d+Au$ and $p+p$ collisions at $\sqrt{s(NN)} = 200$ -GeV*, *Phys. Rev. Lett.* **96** (2006) 012304, [[nucl-ex/0507032](#)].
- [69] B. Z. Kopeliovich, J. Nemchik, I. K. Potashnikova, M. B. Johnson and I. Schmidt, *Breakdown of QCD factorization at large Feynman x* , *Phys. Rev.* **C72** (2005) 054606, [[hep-ph/0501260](#)].
- [70] ATLAS collaboration, G. Aad et al., *Centrality and rapidity dependence of inclusive jet production in $\sqrt{s_{NN}} = 5.02$ TeV proton-lead collisions with the ATLAS detector*, *Phys. Lett.* **B748** (2015) 392–413, [[1412.4092](#)].
- [71] PHENIX collaboration, A. Adare et al., *Centrality-dependent modification of jet-production rates in deuteron-gold collisions at $\sqrt{s_{NN}}=200$ GeV*, *Phys. Rev. Lett.* **116** (2016) 122301, [[1509.04657](#)].
- [72] I. Vitev, *Non-Abelian energy loss in cold nuclear matter*, *Phys. Rev.* **C75** (2007) 064906, [[hep-ph/0703002](#)].
- [73] R. B. Neufeld, I. Vitev and B.-W. Zhang, *A possible determination of the quark radiation length in cold nuclear matter*, *Phys. Lett.* **B704** (2011) 590–595, [[1010.3708](#)].
- [74] S. Dulat, T.-J. Hou, J. Gao, M. Guzzi, J. Huston, P. Nadolsky et al., *New parton distribution functions from a global analysis of quantum chromodynamics*, *Phys. Rev.* **D93** (2016) 033006, [[1506.07443](#)].
- [75] Y.-T. Chien and I. Vitev, *Towards the understanding of jet shapes and cross sections in heavy ion collisions using soft-collinear effective theory*, *JHEP* **05** (2016) 023, [[1509.07257](#)].
- [76] ALICE collaboration, S. Acharya et al., *Constraints on jet quenching in p -Pb collisions at $\sqrt{s_{NN}} = 5.02$ TeV measured by the event-activity dependence of semi-inclusive hadron-jet distributions*, *Phys. Lett.* **B783** (2018) 95–113, [[1712.05603](#)].
- [77] ATLAS collaboration, G. Aad et al., *Measurement of the jet radius and transverse momentum dependence of inclusive jet suppression in lead-lead collisions at $\sqrt{s_{NN}} = 2.76$ TeV with the ATLAS detector*, *Phys. Lett.* **B719** (2013) 220–241, [[1208.1967](#)].
- [78] CMS collaboration, V. Khachatryan et al., *Measurement of inclusive jet cross sections in pp and PbPb collisions at $\sqrt{s_{NN}} = 2.76$ TeV*, *Phys. Rev.* **C96** (2017) 015202, [[1609.05383](#)].
- [79] M. Fickinger, G. Ovanesyan and I. Vitev, *Angular distributions of higher order splitting functions in the vacuum and in dense QCD matter*, *JHEP* **07** (2013) 059, [[1304.3497](#)].
- [80] A. J. Larkoski, I. Moult and D. Neill, *Power Counting to Better Jet Observables*, *JHEP* **12** (2014) 009, [[1409.6298](#)].
- [81] C. Lee, P. Shrivastava and V. Vaidya, *Predictions for energy correlators probing substructure of groomed heavy quark jets*, [1901.09095](#).

- [82] H.-n. Li, Z. Li and C. P. Yuan, *QCD resummation for jet substructures*, *Phys. Rev. Lett.* **107** (2011) 152001, [[1107.4535](#)].
- [83] Y.-T. Chien and I. Vitev, *Jet Shape Resummation Using Soft-Collinear Effective Theory*, *JHEP* **12** (2014) 061, [[1405.4293](#)].
- [84] Z.-B. Kang, F. Ringer and W. J. Waalewijn, *The Energy Distribution of Subjets and the Jet Shape*, *JHEP* **07** (2017) 064, [[1705.05375](#)].
- [85] Z.-B. Kang, F. Ringer and I. Vitev, *Jet substructure using semi-inclusive jet functions in SCET*, *JHEP* **11** (2016) 155, [[1606.07063](#)].
- [86] Z.-B. Kang, X. Liu, F. Ringer and H. Xing, *The transverse momentum distribution of hadrons within jets*, *JHEP* **11** (2017) 068, [[1705.08443](#)].
- [87] Y. Makris and V. Vaidya, *Transverse Momentum Spectra at Threshold for Groomed Heavy Quark Jets*, *JHEP* **10** (2018) 019, [[1807.09805](#)].
- [88] D. P. Anderle, T. Kaufmann, M. Stratmann, F. Ringer and I. Vitev, *Using hadron-in-jet data in a global analysis of D^* fragmentation functions*, *Phys. Rev.* **D96** (2017) 034028, [[1706.09857](#)].